Regular sub-wavelength ripples formation by femtosecond laser pulses on silicon

Yoshiharu Namba, Litao Qi
Motohiro Yasui, Kazuhiro Nishii, Hikoharu Aoki (Brother Industries, LTD.)

In this research, we study the regular sub-wavelength laser induced periodic surface structures (LIPSS) formation on the silicon surface by femtosecond laser pulses. A 780-nm-wavelength femtosecond laser, through a 0.2 mm pinhole aperture for truncating fluence distribution, was focused onto the silicon surface. LIPSS with a spatial period of 710 nm on the entire ablated area are obtained. The initiation and evolution of LIPSS formation are observed by AFM and SEM to well understand the mechanism of LIPSS formation. We find that the ablation mechanism of mass removal before and after the LIPSS formation is changed. Phase explosion play an important role on the mass removal during the LIPSS formation. Depth of regular LIPSS on silicon is measured by AFM and is found to keep a saturated value after regular LIPSS formation. The composition of LIPSS is discussed. Finally, effect of the crystal orientation on the LIPSS formation is evaluated.

1. Introduction

Ultrafast lasers offer a number of advantages in materials processing such as high energy flux and limited thermal effects leading to locally confined structural modification [1]. The semiconductor material silicon is of paramount important in microelectronics [2]. Femtosecond laser ablation of silicon is widely studied due to a number of phenomena concerning photo-induced modification of silicon surfaces, such as ripple formation, column growth and crater formation due to materials removal [3, 4]. Though these phenomena can limit the precision of micromachining, some researches are carried out on the controlled manufactured silicon ripples [5] and microcolumns [6] due to their potential applications such as improvement on the absorptivity and field-emission source in the display technology [7, 8]. High quality micromachining processes by nonthermal ablation are attractive applications of femtosecond lasers but are limited by their low speed manufacturing due to relatively small available average power of the femtosecond laser system, typically several watts. The large area treatments using these phenomena by femtosecond laser pulses are expected to be more practical as the femtosecond fiber laser with high repetition rate is developed.

Ripples formation, also termed laser-induced periodic surface structures (LIPSS) were first observed by Birnbaum on various semiconductor surfaces [9]. Since then, LIPSS on solid materials have been studied extensively [5, 10-13]. The mechanism of LIPSS formation due to the interference between the incident beam and the scatter waves is widely accepted. Recently, self-organization is also proposed as a potential mechanism of LIPSS formation [5] due to the LIPSS similar to the structures induced by ion sputtering [1] and dune formation in desert. Though the physics of ripple formation are studied worldwide, the initiation and growth mechanism still contain unanswered questions. The mechanism of mass removal during femtosecond laser ablation varies with different materials and experimental conditions. Several explanations have been proposed, such as non-thermal ablation [14], direct solid-vapor transition [15], phase explosion [16-18], and Coulomb explosion [19, 20]. The initiation and evolution of LIPSS formation are also affected by the mechanism of mass removal during femtosecond laser ablation. Knowing the mechanism of mass removal during LIPSS formation will be beneficial to understand the mechanism of LIPSS formation and expand their applications. Veld and Veer have reported the initiation of ripples in steel by the femtosecond laser pulses [21]. In this paper, we studied the formation of regular ripples formation on the silicon surface by femtosecond laser pulses. On the ripple formation, we have demonstrated a method to obtain the regular LIPSS on the entire ablated area [22]. In the experiment, the same method is used and regular LIPSS are obtained on the entire ablated area on silicon by femtosecond laser pulses. The process strongly depends on the laser fluence and the number of laser pulses applied to the same spot. The ablation mechanism of mass removal is investigated through observation on the initiation and evolution of LIPSS formation by AFM and SEM. We find that phase explosion play an important role on the mass removal during the LIPSS formation. Depth of regular LIPSS on silicon is measured by AFM and is found to keep a saturated value after regular LIPSS formation. The composition of LIPSS is discussed. Finally, effect of the crystal orientation on the LIPSS formation is evaluated.

2. Experiment

In the experiment, we used a commercially available amplified Ti:sapphire laser system (CyberLaser, IFRIT) that generated 164 fs laser pulses with a maximum pulse energy (E_p) of 1 mJ at a 1 kHz repetition rate and with a central wavelength λ = 780 nm. The horizontally polarized laser beam was focused onto a vertically standing sample at a normal incidence. The samples were mounted on an XYZ-translation stage. The laser beam had a Gaussian profile with a diameter of 6 mm. To obtain a fine periodic ordering of surface nanostructures, the laser beam, through a 0.2 mm pinhole aperture positioned near the 10× objective lens with a NA = 0.3, was focused onto the sample. The laser spot size on the sample was approximately ~10 μm. The maximum pulse energy after the 0.2 mm aperture was 1.038 μJ. The number of laser pulses, N, applied to the sample was controlled by a frequency control system. We studied the initiation and evolution of LIPSS following irradiation with different number of laser pulses. All experiments were carried out in air at atmospheric pressure and room temperature in a cleanroom with Class 100. The material was the silicon wafer [P type, (100) and (111) crystal orientation]. The morphology of the induced periodic structure was examined by scanning electron microscopy (SEM). The surface profile was measured by atomic force microscopy (AFM).

3. Results and discussion

The silicon surface was first irradiated by different pulse energy steps. When the pulse energy is lower than 0.113 μJ, there is no ablation on the irradiated area. The laser fluence of LIPSS formation on silicon by femtosecond laser pulses is around 0.29~0.59 J/cm^2 which is close to the laser fluence to obtain the ripples on the silicon surface by Bonse *et al.* [3]. As the laser fluence increases, microcolumn and the crater are formed on the irradiated area by femtosecond laser pulses.

3.1 LIPSS formation on the entire ablated area

The LIPSS formed on the silicon surface by femtosecond laser pulses with a 0.2 mm aperture following ablation at different number of laser pulses are shown in Fig.1. From the Fig.1, the LIPSS on the entire ablated area are obtained. The orientation of LIPSS is found to be perpendicular to the incident polarization. The mechanism of LIPSS formation due to the interference between the incident beam and the scatter waves has been widely accepted. The

LIPSS formed on the entire ablated area result from the truncated fluence distributions of the laser beam, cutoff in terms of the local fluence and lack of intensity fluctuations [22].

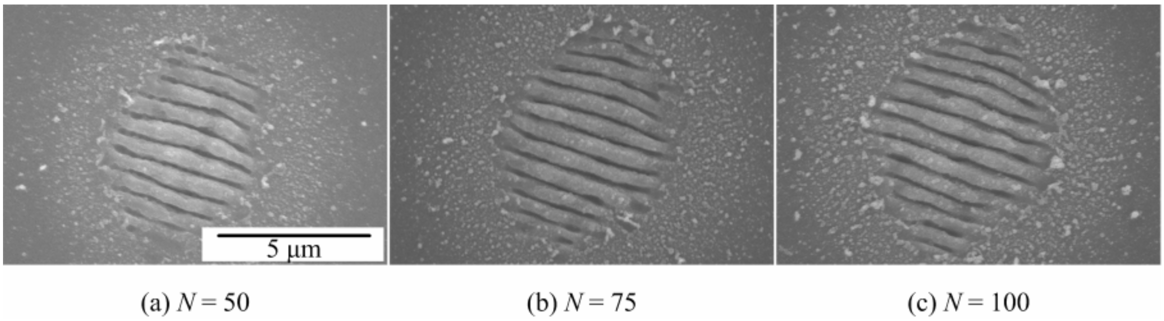

Fig. 1. Regular LIPSS formation on the silicon surface irradiated at E_p = 0.176 μJ and different number of laser pulses.

3.2 Initiation and evolution of LIPSS on silicon

The initiation and evolution of LIPSS on the silicon surface were evaluated by AFM and SEM. Periodic surface structures appeared only after several consecutive pulses, which were found to depend on the type of material, laser fluence, number of laser pulses, and wavelength [3, 13, 22, 23]. Figure 2 shows the evolution of the laser irradiated area by femtosecond laser pulse at E_p = 0.158 μJ and different number of laser pulses. At $N < 10$, no ripples are formed and several rings are observed on the laser irradiated area. The rings formation on the laser irradiated area has been studied by Linde *et al.* and they found that the ablation during the rings formation was characterized as a rapid thermal process and the characteristic states of the conversion of solid material into hot fluid matter [24]. No particles are found around the laser irradiated area during the rings formation. At $10 < N < 25$, the laser irradiated area is characterized by rings(see Fig.2(a) and 2(b)) or ripples (see Fig.2(c) and 2(d)) at intervals under the same experimental conditions. The compared results of the laser irradiated area under the same experimental condition are shown in Fig.3. Two distinct features are existed between the rings and ripples formation. One is the significant change in the ablation depth. The rings have the ablation depth of several nanometer or tens of nanometer (as shown in Fig. 2(a), 2(b), and Fig. 3(a)) and the ripples have the ablation depth of several hundreds of nanometer (as shown in Fig. 2(c), 2(d) and Fig. 3(b)). The other is that a large number of particles are observed around the ripples whereas no particles are found around the rings. The initiation and evolution of ripples on the silicon surface by femtosecond laser pulses are different from that in metals presented by several research groups [21-23]. The initiation and evolution of ripples in metals are the sequence of nanoprotrusions (bubbles), pre-ripples, regular course ripples and regular ripples.

At $N > 25$, the ripples are formed on the entire ablated area and are shown in Fig.4. Then as the laser shot increases, laser induced surface structures entirely fill the ablated area. At $N > 250$ shots, LIPSS start to disappear gradually in the central spot area. At $N = 1000$, LIPSS disappear and microcolumns and microholes are filled with the ablated area. During the formation of LIPSS on the silicon surface by femtosecond laser pulses, large numbers of the particle are observed around the LIPSS. The amount of the particle increases with the number of laser pulses. The particles induced by femtosecond laser irradiation around the LIPSS on the silicon surface are shown in Fig.5. The diameter of the particle is around 100 nm. As the number of laser pulses increased, the particles become larger as shown in Fig. 4(f). Figure 6 shows the evolution of the LIPSS on the ablated areas at different pulse energies and the same laser shots. As the pulse energy increases, periodic patterns, regular LIPSS, and microcolumns are generated on the laser ablated area, sequentially, which are in agreement with the results presented by Bonse *et al.*[3].

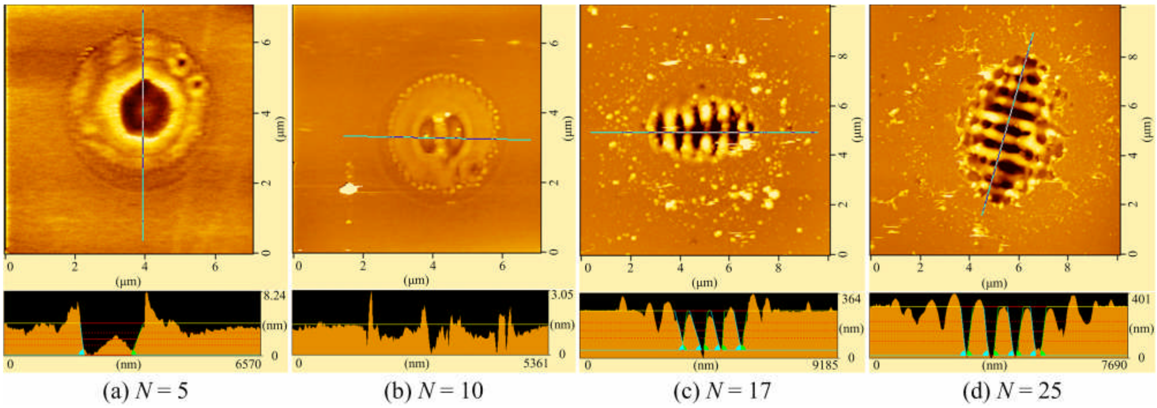

Fig. 2. Evolution of the laser irradiated area by femtosecond laser pulses on the silicon surface at E_p = 0.158 μJ and different number of laser pulses.

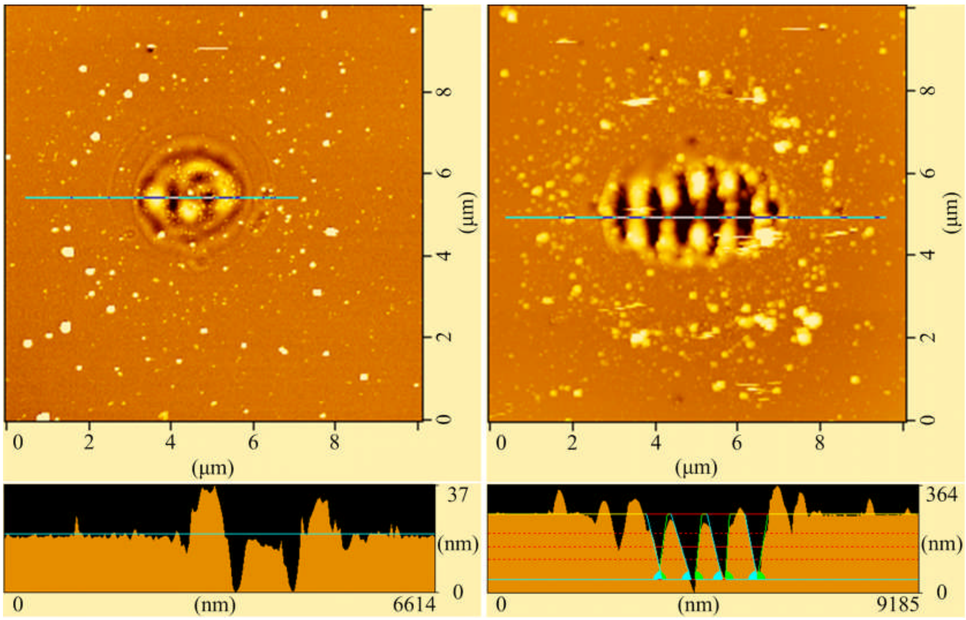

Fig. 3. AFM photos of the laser irradiation area on the silicon surface by femtosecond laser pulses at E_p = 0.158 μJ and N = 17.

3.3 The mechanism of mass removal during the regular LIPSS formation

Phase explosion have been proposed as one of the mechanisms of femtosecond laser ablation of silicon [16, 18]. Cavalleri *et al.* [18] studied the melting and ablation of silicon with time of flight mass spectroscopy and observed several physical processes of thermal melting, nonthermal melting, ablation and plasma formation as the laser fluences increased. Kelly and Miotello [16] studied the contribution of vaporization and boiling to thermal-spike sputtering by laser pulses using a completely classical model of thermal transport in a continuum and identified that phase explosion was the main mechanism of femtosecond laser ablation. In our experiment, the significant change in the ablation depth and large numbers of the particle observation around the LIPSS indicate that a significant mass removal occurs on the laser ablated area on the silicon surface by femtosecond laser pulses during the LIPSS formation. These results suggest that the initiation of a different mechanism or a shift in the primary mechanism responsible for mass removal, which are similar to the results on phase explosion occurring during high power nanosecond laser ablation of silicon [25, 26].

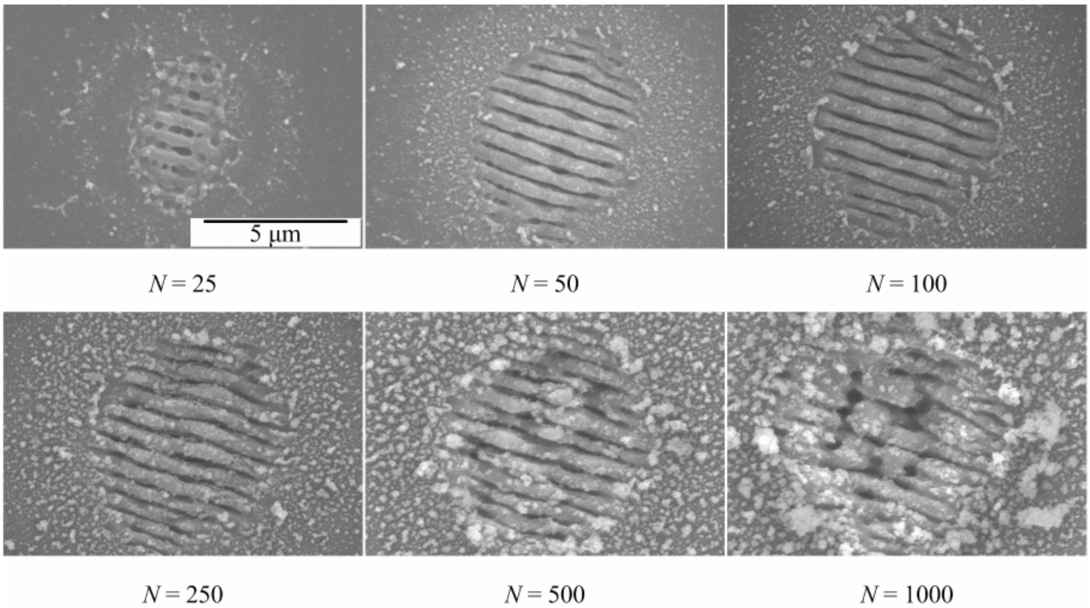

Fig. 4. Evolution of LIPSS on the ablated areas at E_p = 0.176 μJ and different numbers of laser pulses.

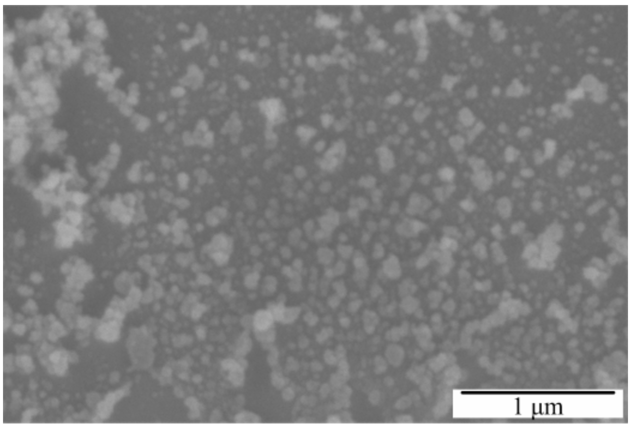

Fig. 5. Particles induced by femtosecond laser irradiation around the LIPSS on the silicon surface at E_p = 0.176 μJ and 50 laser shots.

Cavalleri *et al.* [18] also found the laser fluences for transition from the liquid state to the gas phase ($F_{abl}<F<2F_{abl}$), expansion occurring at temperatures higher than the critical temperature ($F > 2F_{abl}$), and plasma formation ($F > 5F_{abl}$), respectively. The ablation threshold fluences of the Gaussian laser beam can be calculated by measuring the diameter of the ablated areas versus the pulse energy and extrapolating to zero [29]. It is known that for a Gaussian spatial beam profile with a 1/e^2-beam radius, ω_0, the maximum laser fluence, F_0, increases linearly with the laser pulse energy, E_p,

$$F_0 = \frac{2E_p}{\pi\omega_0^2}. \tag{1}$$

The squared diameters, D^2, of the laser ablated craters are correlated with F_0 by [29]

$$D^2 = 2\omega_0^2 \ln\left(\frac{F_0}{F_{th}}\right). \tag{2}$$

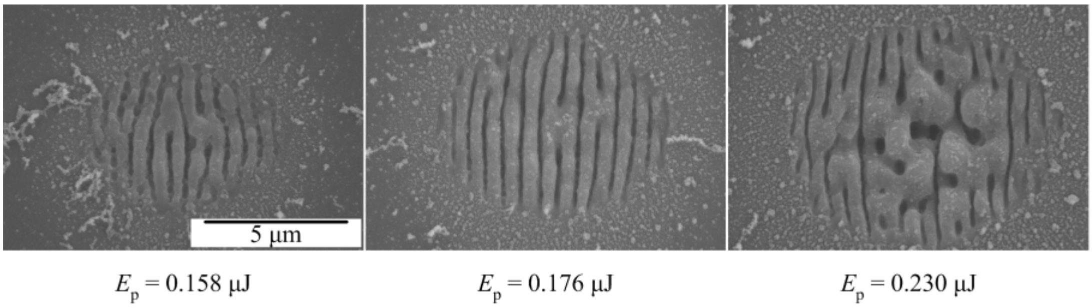

Fig. 6. Evolution of LIPSS on the ablated areas at different pulse energy and 50 laser shots.

Therefore, it is possible to determine the Gaussian beam spot size by measuring the diameters of the ablated area, D, versus the applied pulse energies, E_p. Due to the linearity between energy and maximum laser fluence, a 1/e^2-beam radius of Gaussian beam, ω_0, can be determined by a linear least squares fit in the representation of D^2 as a function of ln(E_p). The Gaussian beam spot size can be obtained. With this value, the maximum laser fluence ϕ_0 could be calculated from the pulse energies in the experiment using Eq. (1). The threshold fluence F_{th} could be obtained by an extrapolation to D^2=0. The result for single pulse laser ablation is shown in Fig. 7. The ablation threshold can be obtained. From the Fig. 7, we obtain a trendlines by linear least squares fit in the representation of D^2 as a function of ln(E_p). The beam spots size and ablation threshold is obtained (see Fig. 7). The ablation threshold fluence of femtosecond laser ablation of silicon by single laser pulse irradiation is 0.26 J/cm^2. The ablation threshold decreases with the number of laser pulses increasing due to the incubation effects [3]. Bonse *et al.* [3] gave a empirical equation between the ablation threshold for N pulses (F(N)) and the ablation threshold for single pulse (F(1))

$$F(N) = F(1)\cdot N^{\zeta-1}. \tag{3}$$

where ξ is a materials-dependent coefficient and is equal to 0.84 during femtosecond laser ablation of silicon obtained by Bonse *et al.* [3]. In our experiment, we obtain the LIPSS on the entire ablated area at N>25. Using the Eq. (3), we can obtain that the ablation threshold fluence of 25 laser shots (F_{abl}(25)) is equal to 0.16 J/cm^2. The laser fluence of LIPSS formation was around 0.29 ~ 0.59 J/cm^2. So we can obtained the relationship between the ablation threshold fluence ($F_{abl}(N)$) and the laser fluence of LIPSS formation (F_{LIPSS}): $1.8F_{abl}(N)<F_{LIPSS}<4F_{abl}(N)$. As the number of laser pulses increases, the laser ablation threshold for N laser shots decreases. It is easy to fulfill the condition of $F_{LIPSS}>2F_{abl}(N)$ which corresponds with the results that expansion occurring at temperature higher than the critical temperature presented by Cavalleri *et al.* [18]. From the analysis of the experimental results, we confer that phase explosion is the main mechanism of femtosecond laser ablation of silicon during regular LIPSS formation. It is to be stressed that homogeneous boiling (phase explosion) occurs over the whole liquid layer and not only the surface as heterogeneous boiling [18, 27, 28]. It is easy to understand the significant change in ablation depth before and after the ripple formation. The significant change in ablation depth during the ripple formation is due to the phase explosion occurring over the whole liquid layer, while the thinner ablation depth during the ring formation is due to the normal boiling or vaporization only occurring over the surface of the laser irradiated area.

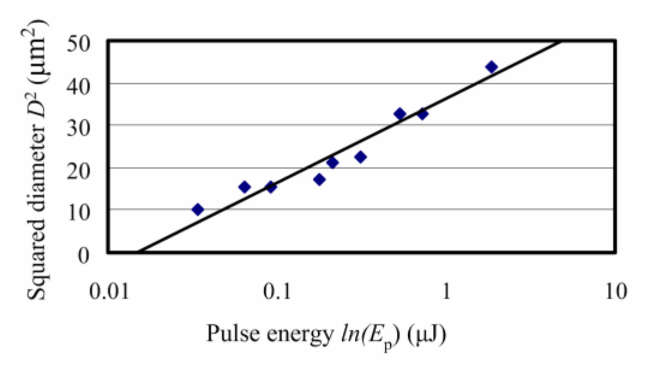

Fig. 7. Squared diameter D^2 of the ablated area versus the applied pulse energy E_p on femtosecond laser ablation of silicon by single laser pulse irradiation.

3.4 Spatial period and depth of LIPSS formed on silicon

The profile of regular LIPSS on the silicon surface is shown in Fig. 8. The typical feature size of regular LIPSS is around 710 nm. The spatial period of LIPSS does not precisely correspond to the laser wavelength and is a little smaller than the laser wavelength. The deviation of the spatial period from the laser wavelength was attributed to the optic parameter variation due to the surface plasmons excited by the femtosecond laser irradiation of the surface [23]. The LIPSS formation on the silicon surface has the same level with the surface of the sample, as shown in Fig. 8; whereas, the LIPSS formation on the stainless steel surface with a depth of about 250 nm was on the surface of the ablated crater with a depth of about 700 nm [22]. The compared results of LIPSS formation on the silicon and stainless steel surface by femtosecond laser pulses is shown in Fig. 9. The formation of LIPSS is attributed to the interference between the incident light and a surface wave (generated by scattering). This interference leads to periodic modulation of the absorbed intensity and consequently to modulated ablation. But the LIPSS formation on different materials also has relevance of the mechanism of femtosecond laser ablation of different materials.

Until now, more researches are focused on the spatial period of the LIPSS. LIPSS with a spatial period much smaller than the laser wavelength on different materials by femtosecond laser pulses have been reported [13, 22, 30-35]. However, few researches are carried out on finding the relationship between the depth of LIPSS and the applied parameters. Normally, it is difficult to obtain the depth of LIPSS which is sensitive to the pulse energy and the number of laser pulses or only emerged at the edge the ablated craters. Regular LIPSS formed on the entire ablated area is obtained in our experiment and then the depth of LIPSS on silicon is measured by AFM. Regular LIPSS formation is very sensitive to the pulse energy, as shown in

Fig.6. Only the depth of the LIPSS on the silicon surface varying with the number of laser pulses is presented, as shown in Fig.10. After 25 laser shots, the depths of regular LIPSS on the silicon surface are around 362 ± 17 nm. Normally, the depths of the ablated crater by femtosecond laser pulses increase with the number of laser pulses [36]. However, the depths of regular LIPSS on silicon by femtosecond laser pulses keep a saturated value after N >25. On the femtosecond laser ablation (or irradiation) of silicon, there are some special features. For example, Izawa *et al.* found a ultrathin amorphous Si layer formed by femtosecond laser pulse irradiation at low laser fluence and was quite uniform and did not depend on the laser fluence and the number of irradiated laser pulses [37]; Rogers *et al.* found that the amorphous Si layer inside the craters ablated by high power femtosecond laser pulses was absent and a layer of a defective single crystalline Si was observed and was 400 nm thick on average with a standard deviation of 200 nm [38]. Further experiments to clarify the relationship between the depth of regular LIPSS and the subdamage lay will be carried out using TEM. More investigations on the depth of LIPSS will be beneficial to well understand the mechanism of LIPSS formation and expand the applications of LIPSS. The amorphous Si layer contribution was weak and the polymorphs Si layer was dominated on the ripples zone [5]. In our experiment, we find regular LIPSS after an ultrasonic cleaning become unclear and irregular. Further experiments on the composition of LIPSS are being carried out and the results are useful to understand the role of the self-organization mechanism in the LIPSS formation on silicon by femtosecond laser pulses.

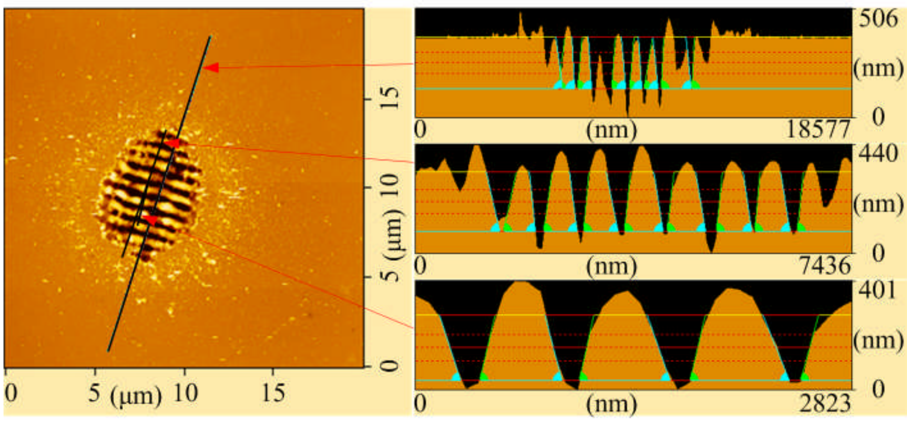

Fig.8. AFM photos of section profile of LIPSS on the silicon surface by femtosecond laser pulses at E_p = 0.176 μJ and N = 25.

3.5 LIPSS formation on different crystal orientation of silicon

Experiment on the crystal orientation dependence of LIPSS formation on (100) and (111) Si was carried out. The results show that the formation of LIPSS is independent of the crystal orientation. The same result was reported by Borowiec and Haugen on the experiments on the crystal orientation dependence of LIPSS formation on (100) and (110) GaAs [13]. From our experiment, it is difficult to obtain the effect of the crystal orientation on the mechanism of LIPSS formation. But the LIPSS formation independent of the crystal orientation could be partially explained from the point in the mass removal. We carried out the experiments on the effect of the crystal orientation on the diameter and ablation depth of the craters by femtosecond single laser pulses on silicon. The results show that the crystal orientation has little effects on the diameter and the depth of the ablated crater when the laser fluence is below 5.42 J/cm^2, as shown in Fig.11 and Fig.12.

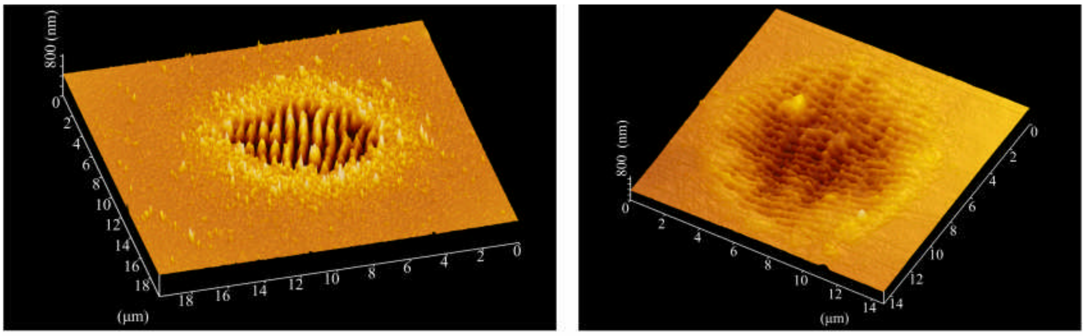

(a) Silicon wafer, $E_p = 0.176$ μJ and $N = 75$, focus: 10× with NA = 0.30.

(b) Stainless steel, $E_p = 1.04$ μJ and $N = 25$, focus: 5× with NA = 0.15.

Fig.9. AFM photos of 3D profiles of LIPSS formation on the silicon and stainless steel surfaces by femtosecond laser pulses.

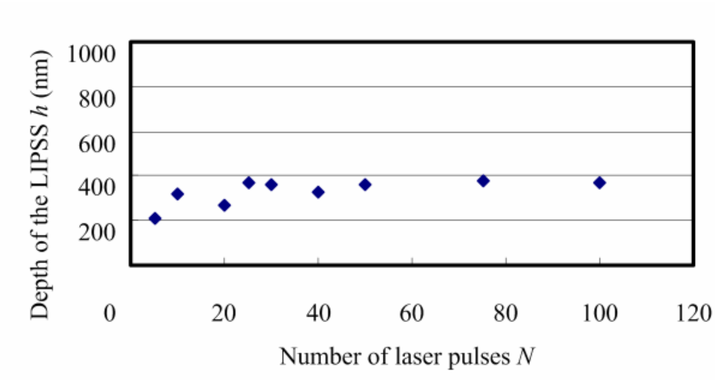

Fig.10. Relationship between the depth of regular LIPSS and the number of laser pulses on the silicon surface by femtosecond laser pulses at E_p = 0.176 μJ.

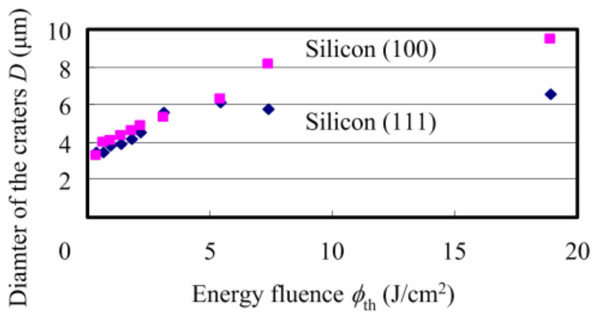

Fig.11. Relationship between the diameter of the ablated craters and the laser fluence by single femtosecond laser pulse irradiation on different crystal orientation of silicon.

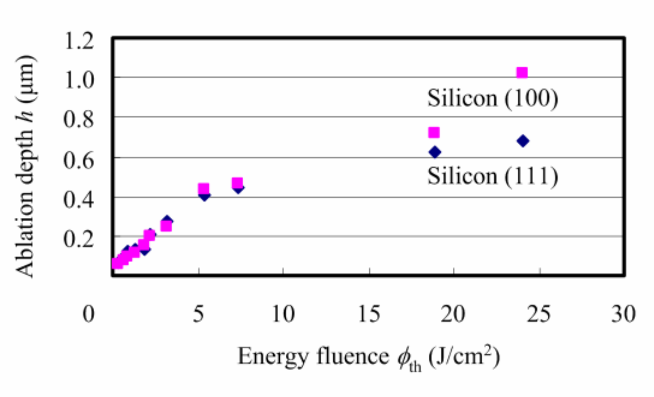

Fig. 12. Relationship between the ablation depth of the ablated craters and the laser fluence by single femtosecond laser pulse irradiation on different crystal orientation of silicon.

4. Conclusions

Experiments on regular LIPSS formation on the silicon surface by femtosecond laser pulses were carried out. The mechanism of LIPSS formation by femtosecond laser pulses was discussed. The main conclusions are as follows:

1) Regular LIPSS with a spatial period of about 710 nm on the entire ablated area are obtained. The LIPSS on the entire ablated area result from the truncated fluence distributions of the laser beam, cutoff in terms of the local fluence and lack of intensity fluctuations
2) On initiation an evolution of LIPSS on silicon, the rings and ripples form in intervals on the laser irradiated area when few numbers of laser pulses are used at low laser fluence. Two distinct features are existed between the rings and ripples formation: a significant change in the ablation depth and large number of the particle generation, which means the initiation of a different mechanism or a shift in the primary mechanism responsible for mass removal.
3) We confer that the ablation mechanism for mass removal is the phase explosion during LIPSS formation on silicon by femtosecond laser pulses. The laser fluence for the LIPSS formation (F_{LIPSS}) has the following relationship with the laser ablation threshold fluence (F_{abl}): $1.8F_{abl} < F_{LIPSS} < 4F_{abl}$, which meets the conditions for phase explosion occurring and avoids plasma generation.
4) Depth of LIPSS on silicon by femtosecond laser pulses keeps a saturated value when regular LIPSS are formed on the entire ablation area.
5) The formation of regular LIPSS on silicon by femtosecond laser pulses is independent of the crystal orientation.

References

1) J. Perrière, E. Millon and E. Fogarassy: Recent advances in laser processing of materials (Elsevier Science, 2006).
2) G. Harbeke and M. J. Schulz: Semiconductor silicon: materials science and technology (Springer-Verlag, 1989).
3) J. Bonse, S. Baudach, J. Krüger, W. Kautek, and M. Lenzner: Femtosecond laser ablation of silicon-modification thresholds and morphology, Appl. Phys. A, **74**, (2002) p. 19-25.
4) E. Coyne, J. Magee, P. Mannion, and G. O' Connor: A study of femtosecond laser interaction with wafer grade silicon, Proc. SPIE, **4876**, (2003) p. 487-499.

5) F. Costache, S. Kouteva-Arguirova, and J. Reif: Sub-damage-threshold femtosecond laser ablation from crystalline Si: surface nanostructures and phase transformation, Appl. Phys. A, **79,** (2004) p. 1429-1432.
6) T. H. Her, R. J. Finlay, C. Wu, and E. Mazur: Femtosecond laser-induced formation of spikes on silicon, Appl. Phys. A, **70,** (2000) p. 383-385.
7) A. S. Mahmood, M. Sivakumar, K. Venkatakrishnan, and B. Tan: Enhancement in optical absorption of silicon fibrous nanostructure produced using femtosecond laser ablation, Appl. Phys. Lett., **95,** (2009) p. 034107.
8) A. Y. Vorobyev and C. Guo: Effects of nanostructure-covered femtosecond laser-induced periodic surface structures on optical absorptance of metals, Appl. Phys. A (Rapid Comm.), **86,** (2007) p. 321-324.
9) M. Birnbaum: Semiconductor Surface Damage Produced by Ruby Lasers, J. Appl. Phys., **36,** (1965) p. 3688-3689.
10) P. M. Fauchet and A. E. Siegman: Surface ripples on silicon and gallium arsenide under picosecond laser illumination, Appl. Phys. Lett., **40,** (1982) p. 824-826.
11) G. S. Zhou, P. M. Fauchet, and A. E. Siegman: Growth of spontaneous periodic surface structures on solids during laser illumination, Phys. Rev. B, **26,** (1982) p. 5366-5381.
12) J. F. Young, J. S. Preston, H. M. van Driel, and J. E. Sipe: Laser-induced periodic surface structures. II. Experiment on Ge, Si, Al, and brass, Phys. Rev. B, **27,** (1983) p. 1155-1172.
13) A. Borowiec and H. K. Haugen: Subwavelength ripple formation on the surfaces of compound semiconductors irradiated with femtosecond laser pulses, Appl. Phys. Lett., **82,** (2003) p. 4462-4464.
14) J. Yang, Y. Zhao, and X. Zhu: Transition between nonthermal and thermal ablation of metallic targets under the strike of high-fluence ultrashort laser pulses, Appl. Phys. Lett., **88,** (2006) p. 094101.
15) B. N. Chichkov, C. Momma, S. Nolte, F. von Alvensleben, and A. Tünnermann: Femtosecond, picosecond and nanosecond laser ablation of solids, Appl. Phys. A, **63,** (1996) p. 109-115.
16) A. Miotello and R. Kelly, Contribution of vaporization and boiling to thermal-spike sputtering by ions or laser pulses, Phys. Rev. E, **60,** (1999) p. 2616-2625.
17) N. M. Bulgakova and I. M. Bourakov: Phase explosion under ultrashort pulsed laser ablation: modeling with analysis of metastable state of melt, Appl. Surf. Sci., **197-198,** (2002) p. 41-44.
18) A. Cavalleri, K. Sokolowski-Tinten, J. Bialkowski, M. Schreiner, and D. Linde: Femtosecond melting and ablation of semiconductors studied with time of flight mass spectroscopy, J. Appl. Phys., **85,** (1999) p. 3301-3309.
19) W. G. Roeterdink, L. B. F. Juurlink, O. P. H. Vaughan, J. D. Diez, M. Bonn, and A. W. Kleyn: Coulomb explosion in femtosecond laser ablation of Si(111), Appl. Phys. Lett., **82,** (2003) p. 4190-4192.
20) R. Stoian, D. Ashkenasi, A. Rosenfeld, and E. E. B. Campbell: Coulomb explosion in ultrashort pulsed laser ablation of Al_2O_3, Phys. Rev. B, **62,** (2000) p. 13167-13173.
21) B. H. Veld and H. Veer: Initiation of femtosecond laser machined ripples in steel observed by scanning helium ion microscopy, J. Laser Micro/Nanoeng., **5,** (2010) p. 28-34.
22) L. Qi, K. Nishii, and Y. Namba: Regular subwavelength surface structures induced by femtosecond laser pulses on stainless steel, Opt. Lett., **34,** (2009) p. 1846-1848.
23) A.V. Vorobyev, V. S. Makin, and C. L. Guo: Periodic ordering of random surface nanostructures induced by femtosecond laser pulses on metals, J. Appl. Phys., **101,** (2007) p. 034903.
24) K. Sokolowski-Tinten, J.Bialkowski, A. Cavalleri, D. von der Linde, A. Oparin, J.

Meyer-ter-Vehn, and S. I. Anisimov: Transient states of matter during short pulse laser ablation, Phys. Rev. Lett., **81,** (1998)p.224-227.
25) J. H. Yoo, S. H. Jeong, R. Greif, and R. E. Russo: Explosive change in crater properties during high power nanosecond laser ablation of silicon, J. Appl. Phys., **88,** (2000)p.1638-1649.
26) Q. Lu, S. S. Mao, X. Mao, and R. E. Russo: Delayed phase explosion during high-power nanosecond laser ablation of silicon, Appl. Phys. Lett., **80,** (2002)p.3072-3074.
27) A. Miotello and R. Kelly: Critical assessment of thermal models for laser sputtering at high fluences, Appl. Phys. Lett., **67,** (1995)p.3535-3537.
28) A. Peterlongo, A. Miotello, and R. Kelly: Laser-pulse sputtering of aluminum: Vaporization, boiling, superheating, and gas-dynamic effects, Phys. Rev. E, **50,** (1994)p.4716- 4727.
29) J. M. Liu: Simple technique for measurements of pulsed Gaussian-beam spot sizes, Opt. Lett., **7,** (1982)p.96-198.
30) R. Wagner and J. Gottmann: Sub-wavelength ripple formation on various materials induced by tightly focused femtosecond laser radiation, J. Phys.: Conference Series, **59,** (2007) p.333-337.
31) A. Weck, T. H. R. Crawford, D. S. Wilkinson, H. K. Haugen, and J. S. Preston: Ripple formation during deep hole drilling in copper with ultrashort laser pulses, Appl. Phys. A, **89,** (2007)p.1001-1003.
32) R. Le Harzic, H. Schuck, D. Sauer, T. Anhut, I. Riemann, and K. König: Sub-100 nm nanostructuring of silicon by ultrashort laser pulses, Opt. Express, **13,** (2005)p.6651-6656.
33) A. M. Ozkan, A. P. Malshe, T. A. Railkar, W. D. Brown, M. D. Shirk, and P. A. Molian: Femtosecond laser-induced periodic structure writing on diamond crystals and microclusters, Appl. Phys. Lett., **75,** (1999)p.3716-3718.
34) N. Yasumaru, K. Miyazaki, and J. Kiuchi: Femtosecond-laser-induced nanostructure formed on hard thin films of TiN and DLC, Appl. Phys. A, **76,** (2003)p.983-985.
35) M. Shinoda, R. R. Gattass, and E. Mazur: Femtosecond laser-induced formation of nanometer-width grooves on synthetic single-crystal diamond surfaces, J. Appl. Phys., **105,** (2009)p.053102.
36) X. Zeng, X. Mao, R. Greif and R. E. Russo: Ultraviolet femtosecond and nanosecond laser ablation of silicon: ablation efficiency and laser-induced plasma expansion, Proc. SPIE, **5448,** (2004)p.1150-1158.
37) Y. Izawa, Y. Izawa, Y. Setsuhara, M. Hashida, M. Fujita, R. Sasaki, H. Nagai, and M. Yoshida: Ultrathin amorphous Si layer formation by femtosecond laser pulse irradiation, Appl. Phys. Lett., **90,** (2007)p.044107.
38) M. S. Rogers, C. P. Grigoropoulos, A. M. Minor and S. S. Mao: Absence of amorphous phase in high power femtosecond laser-ablated silicon, Appl. Phys. Lett., **94,** (2009)p.011111.